A Novel Simple Current-mode Square/Triangular Wave Generator with Independently-Linearly Controllable Frequency and Amplitudes

Montree Siripruchyanun
Department of Teacher Training in Electrical Engineering, Faculty of Technical Education,
King Mongkut's Institute of Technology North Bangkok, Bangkok, 10800, THAILAND
Email: mts@kmitnb.ac.th

Abstract

In this paper, a current-mode square/triangular wave is presented. Due to operation in current-mode, the proposed circuit provides a wide frequency response, a low supply voltage, low power consumption and electronic controllability. Thus, it is very suitable for use in portable and battery-powered equipments. The proposed square/triangular wave generator consists of merely current mode Schmitt trigger and current mode integrator with current squarer, which can be fabricated into Integrated Circuit (IC) form through a CMOS technology. The features of the proposed circuit is that it can provide simultaneously both a square wave and a triangular wave whose frequency and amplitudes can be independently controlled by input bias currents. The performances of the proposed circuit are explored through HSPICE simulation program using BSIM3v3 parameters of AMIS 0.5μm, they demonstrate good agreement to the theoretical anticipation. The proposed circuit works at as low as ±1V supply voltages; power consumption is merely 10.9μW.

Keywords: Signal generator, Current-mode, CMOS

1. Introduction

Voltage/Current Controlled Oscillators (VCOs/CCOs) play important roles in many fields such as instrumentation, electronic and communication systems. The VCO based on OTA has been proposed [1]. Its advantage is that the oscillation frequency is independent of the temperature. However, it has much a complicated scheme and a small range of the oscillation frequency due to comprising of operational amplifiers, which have narrow bandwidth relative to an OTA [2]. Especially the amplitude adjustments of square/triangular wave can not be achieved. Recently, current controlled oscillator over a wide range has been introduced [3], this circuit performs square/triangular waves with electronic controllability only frequency, not include its amplitudes. Hence, these schemes still do not provide sufficient stability to implement them as a precise component in the design of instrumentation and communication systems, particularly under varying environment conditions. Besides, most of literatures consume high supply voltage and power consumption.

In the last decade, there has been much effort to reduce the supply voltage of an analog CMOS system. This is due to the command for portable and battery-powered equipment. Since a low-voltage operating circuit becomes necessary, the current–mode technique is ideally suited for this purpose [4]. Unfortunately, most of previous square/triangular wave generators work in voltage-mode, which is not suitable for working in a current-mode signal processing system.

The purpose of this article is to present a realization of a novel square/triangular wave generator functioning in current-mode. The proposed circuit comprises current controllable current-mode Schmitt trigger and current-mode integrator. All circuits can be realized using a standard CMOS technology. The simulation results through HSPICE using BSIM3v3 model of AMIS 0.5μm are achieved to confirm that the realized circuit can provide a wide dynamic range, a low supply voltage, a wide bandwidth including low-power consumption. In addition, the output frequency and amplitudes can be independently-linearly tuned through input bias currents. Consequently, the proposed circuit is very appropriate for further fabricating into Integrated Circuit (IC) form to employ in the current-mode signal processing system.

2. Circuit Principle and Description

2.1 The Proposed Principle

The proposed square/triangular wave generator is composed of 3 main parts, illustrated in Fig. 1. Current-mode Schmitt trigger is employed to change a triangular wave to a square wave, which is fed-back as input signal to current-mode integrator. A current squarer is employed to make the integrator able to linearly control of frequency. As briefly explained, the current-mode square wave can be achieved at the output of the Schmitt trigger while the current-mode triangular wave can be obtained at the output of the integrator.

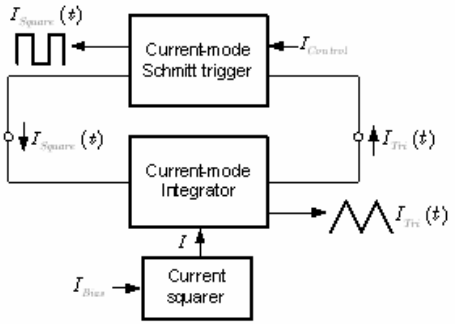

Fig. 1: Proposed principle

2.2 Circuit Description and Operation

Fig. 2 shows circuit details of the current squarer [5]. The current-mode Schmitt trigger, shown in Fig. 3

EL050

[6], whose transfer characteristic can be found in Fig. 4. If the aspect ratios of the MOS transistors are set to appropriate values, it can be found that both output current and threshold current can be adjusted by a control current: $I_{Control}$. The circuit description of the current-mode integrator is shown in Fig. 5 [7]. From straightforward analysis, the output current of the integrator: $I_{Tri}(t)$ can be obtained by

$$I_{Tri}(t) = \frac{Kg_m}{C}\int_0^t I_{Square}(t) \qquad (1)$$

where K is an arbitrary value dependent on current source KI and aspect ratio of M16.

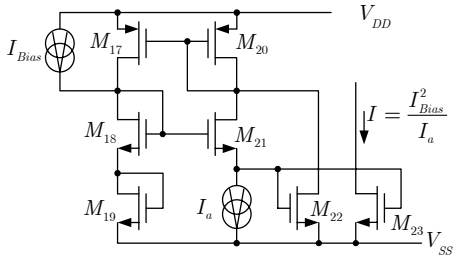

Fig. 2: Current squarer

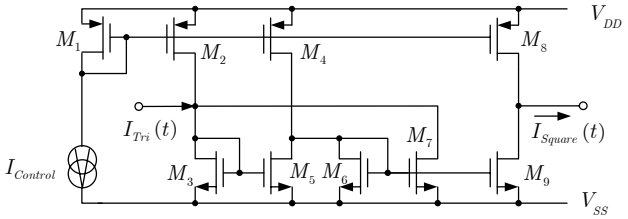

Fig. 3: Current-mode Schmitt trigger

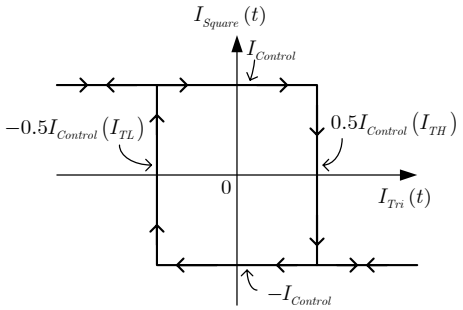

Fig. 4: Transfer characteristic of Schmitt trigger in Fig. 2

Period (T) of output signals can be easily achieved from Eqn. (1) by

$$I_{Control} = \frac{Kg_m}{C}\int_0^{T/2} I_{Control}dt\,. \qquad (2)$$

Consequently, it is found that

$$T = \frac{2C}{Kg_m}. \qquad (3)$$

The oscillation frequency (f_o) can be subsequently identified by

$$f_o = \frac{Kg_m}{2C} = \frac{K\sqrt{2\mu_n C_{ox}\frac{W}{L}I}}{2C} = \frac{K'I_{Bias}}{C} \qquad (4)$$

where $I = \frac{I_{Bias}^2}{I_a}$, $K' = K\sqrt{2\mu_n C_{ox}\frac{W}{L}I_a}/2$ and I_a is a constant current. From Eqn. (4), it is obviously seen that the oscillation frequency can be adjusted by either the bias current: I_{Bias} or capacitor: C. In addition, it is theoretically independent of supply voltage.

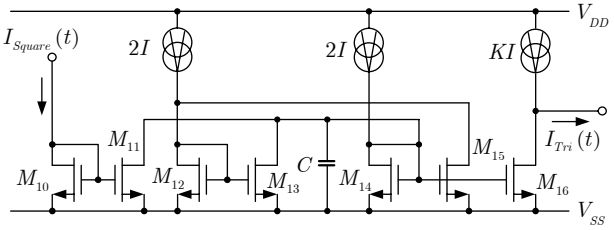

Fig. 5: Current-mode integrator

The output amplitudes of triangular and square wave will be respectively equal to

$$I_{Tri(P-P)} = I_{Control} \qquad (5)$$

$$I_{Square(P-P)} = 2I_{Control}\,. \qquad (6)$$

It can be seen that, from Eqns. (4)-(6), the output frequency and amplitudes can be independently controlled trough I_{Bias} and $I_{Control}$, respectively.

3. Circuit Performance Analysis

3.1 Effect of the DC offset current

The DC offset current of the current-mode Schmitt trigger affects the operation of the oscillator. Let us consider an offset current: $\pm I_{off}$, which is effective on the charge or discharge current of the timing capacitor in the integrator. Thus, Eqn. (3) is modified to

$$T = \frac{2C}{Kg_m}\left(\frac{1}{1-\frac{I_{off}^2}{I_{Control}^2}}\right). \qquad (7)$$

Similarly, the output frequency is changed to

$$f_o = K'\frac{I_{Bias}}{C}\left(1-\frac{I_{off}^2}{I_{Control}^2}\right). \qquad (8)$$

For small offset current $\left(I_{off}/I_{Control} \ll 1\right)$, from Eqn. (8), the influence of the DC offset current on the oscillation frequency can be negligible.

3.2 High-frequency capability

The switching delays within the circuit limit the high-frequency capability of the oscillator. These delays are the results of the switch speeds of MOS devices, the internal current levels, and the parasitic capacitances. In an actual design, a switching-time delay: t_s is involved during the current reversal [8].

From the above analysis, one can derive an actual frequency: f_a expression of the form

$$f_a = f_o \frac{1}{1 + f_o t_s \gamma}. \quad (9)$$

The constant γ is in the range of $2 \le \gamma \le 4$, where the upper and lower limits on γ correspond to cases

(a) The charging current continues to flow and is not reversed until the completion of switching time t_s. This results a time delay of $2t_s$.

(b) The charging current stops at the beginning of the switching cycle and is reversed at the completion of switching time. This results a time delay t_s.

Therefore, it is possible to define a theoretical maximum frequency of oscillation: f_{max}, limited only by the switching time delays as

$$f_{\max} = \frac{1}{\gamma t_s}. \quad (10)$$

From a practical point of view, frequency accuracy and temperature stability requirements limit the useful range of the oscillator to frequencies that are on the order of 10-20% of f_{max}.

3.3 The frequency stability

The oscillator confronts several contributing factors, which affect the temperature stability

(a) Stability of internal charge and discharge currents with temperature

(b) Stability of Schmitt trigger thresholds

(c) Temperature coefficient of switching delays

For the oscillation frequencies $f_o t_s \gamma \ll 1$, Eqn. (9) can be approximated as

$$f_a = f_o \left(1 - f_o t_s \gamma\right). \quad (11)$$

Differentiating this equation with respect to temperature

$$\frac{1}{f_a}\frac{\partial f_a}{\partial T} = -\frac{f_o}{f_{\max}}\frac{1}{t_s}\frac{\partial t_s}{\partial T}. \quad (12)$$

Switching delays exhibit a positive temperature coefficient, therefore even at frequencies equal to 10% of $f_{\max}$, the switching delays contribute a negative temperature coefficient to the oscillation frequency.

Conclusions of the above mentioned discussion are that; for low frequencies, switching delays are negligible and the frequency stability at high frequencies is determined by switching delays within the oscillator feedback loop.

4. Simulation Results and Discussion

The proposed square/triangular wave generator was simulated using HSPICE through AMIS 0.5µm CMOS technology BSIM3v3 model parameters. The aspect ratios of all transistors are listed in Table 1. The circuit was operated with ±1V supply. The output waveforms of the square/triangular wave generator for $I_{Control}$ = 1µA, I_{Bias} = 1µA, I_a = 5µA and C = 10nF are shown in Fig. 6, and for $I_{Control}$ = 1 µA, I_{Bias} = 1µA, I_a = 1µA and C = 0.1nF are shown in Fig. 7. From Fig. 7, it can be observed that the triangular wave amplitude is higher than that of in Fig. 6, which is due to the switching-time delay, as explained in Section 3.

Table 1: Transistor Aspect Ratio

Transistor	W/L (µm/µm)
M1, M8	20/2.4
M2	50/2.4
M4	40/2.4
M3, M5, M6, M9	15/1.2
M7	20/1.2
M10 - M15, M17, M20	20/3
M16	20/3 (M=5)
M21-M22	10/3
M18, M19, M23	10/3 (M=4)

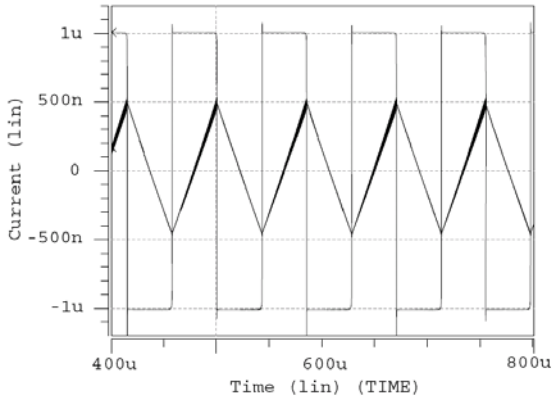

Fig. 6: Low Frequency Output waveforms (f_o = 13kHz)

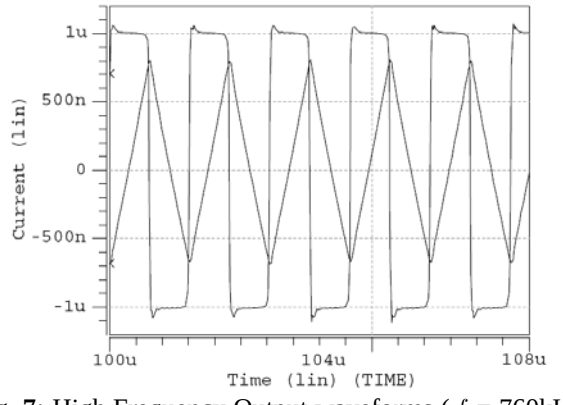

Fig. 7: High Frequency Output waveforms (f_o = 760kHz)

EL050

Fig. 8 illustrates the frequency of oscillations, when current I_{Bias} is varied, for $I_{Control}$ = 1μA, I_a = 1μA and C = 5, 7.5 and 10nF. In addition, the frequency deviations due to variations of supply voltages are also investigated, shown in Fig. 9. It shows that the frequency is dependent on supply voltage due to performance of the integrator. Fig. 10 depicts the frequency deviations due to temperature variations from 0 to 100°C, where frequency is set to 100kHz at the room temperature (27°C). It shows that the absolute maximum deviation is merely 9.1%. These deviations derive from the circuit performances, as explained in Section 3. The maximum consumed power is about 10.9μW.

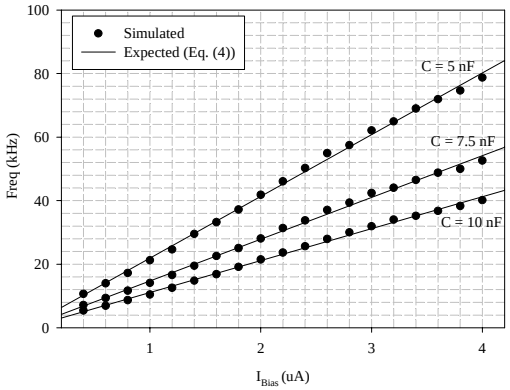

Fig. 8: Frequency of oscillation versus bias current

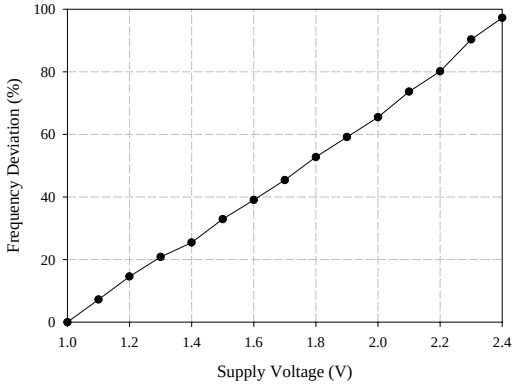

Fig. 9: The frequency deviations due to supply voltages

5. Conclusion

A new square/triangular wave generator has been introduced. The realized circuit shows good performances, in which the oscillation frequency and output amplitudes can be independently controlled by input bias currents. The linear control of oscillation frequency can be achieved by employing a current squarer. The simulation results obtained from HSPICE confirm the theoretical anticipations, while the maximum frequency is up to 100MHz range. It is also found that the circuit can work at low-supply voltage (±1V) and low-power consumption (10.9μW). Consequently, the proposed circuit is very suitable for further implementing in integrated circuit to employ in a current-mode signal processing system.

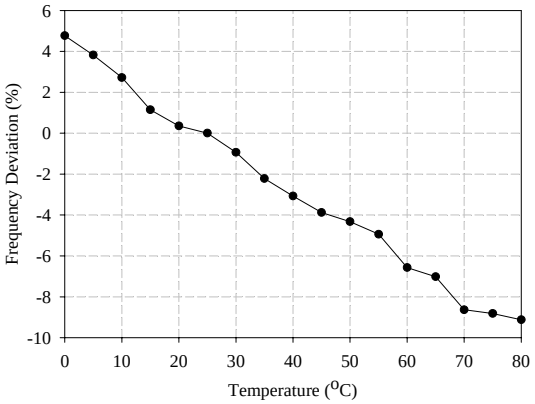

Fig. 10: Frequency deviations due to temperature drift

6. Acknowledgement

The author would like to thank Mr. Kriangkrai Sooksood for his help to prepare paper and simulation.

7. References

[1] J. W. Haslett "Current – Switching VCO", Elec. Letters, vol. 25, no. 2, pp. 139-140, Jan. 1989.

[2] W. S. Chung, and Cha, K.H. Kim "Temperature-stable VCO based on operational transconductance amplifiers", Elec. Letters, vol. 26, no. 22, pp. 1900-1901, Oct. 1990.

[3] O. Cicekoglu, and A. Toker, "Current mode oscillator with linear period control over a wide range", Int. J. Electronics, vol. 86, no. 12, pp. 1453-1462, 1999.

[4] C. Toumarzou, F.J. Lidgey and D.G. Haigh, Analogue IC design: the current-mode approach, Peter Peregrinus, London, UK., 1990, Ch. 1.

[5] E. S. Sinencio and A. G. Andreou (editors), Low-voltage/low-power integrated circuits and systems: low-voltage mixed-signal circuits, IEEE press, New York, 1999, Ch. 4.

[6] A. L. Coban and P. E. Allen, "A Low-voltage Current-mode Schmitt trigger implemented in standard CMOS technology", Proc. ICM'94, pp. 172-175, Sept. 1994.

[7] S. S. Lee, R. H. Zele, D. J. Allstot and G. Liang, "A Continuous-time Current-mode Integrator", IEEE Tran. on Circuits and Systems, Vol. 38, No. 10, pp. 1236-1238, Oct. 1991.

[8] A. B. Grebene, Bipolar and MOS analog integrated circuit design, NY, John Wiley, pp. 556-591, 1984.